COMPUTATION OF RESISTIVE WALL WAKEFIELDS WITH THE PBCI CODE

R. Mäkinen*, Tampere University of Technology, Department of Electronics,
P.O. Box 692, 33101 Tampere, Finland
T. Lau#, E. Gjonaj, T. Weiland, Technische Universität Darmstadt, TEMF,
Schlossgartenstrasse 8, 64289 Darmstadt, Germany.

Abstract

Wakefield effects due to arbitrary 3D geometries can be estimated with the Parallel Beam Cavity Interaction (PBCI), a parallelized and dispersion-free code. However, resistive wall losses may also have a significant effect on the beam line impedance. The contribution of this work is to incorporate these losses into PBCI simulations using wide band surface-impedance boundary conditions. The developed models are validated by convergence studies and by wakefield simulations with selected test structures.

INTRODUCTION

Numerical techniques are usually required to determine short-range wakefields and potentials of ultra-short electron bunches in complex accelerator components. The PBCI code [1] is a massively parallelized, fully 3D, explicit time-domain code for the wakefield computations in arbitrary accelerator structures. The spatial discretization is based on the Finite Integration Technique (FIT) [2]. A longitudinal-transverse (LT) split-operator scheme [3] ensures dispersion-free propagation in the longitudinal direction allowing accurate modelling of micrometer-scale details as part of the electrically large accelerator structures. The longitudinal numerical phase velocity exactly matches the analytic speed of light allowing implementation of a moving window tracking the bunch. Computational efficiency is increased by a frequency-domain reconstruction of the wakefield solution for finite homogeneous beam pipes connecting the structures, alleviating the need for their inclusion in time-domain simulation.

The resistive wall loss of accelerator structures may be a significant source for impedance. This is in particular the case e.g. for the coated collimators used in the ILC-ESA test beam experiments [4]. In this work, a first-order surface-impedance boundary condition (SIBC) is implemented for the LT scheme. The surface-impedance function is approximated in the frequency domain by rational functions and transformed into time domain [3]. A wide-band approximation up to 100 THz is required to model ultra-short particle bunches. The SIBC formulation for standard FIT computations has been previously reported (see [5], [6]). In the present work, appropriate SIBCs are developed for the LT split-operator scheme in the framework of wakefield computations.

* R. Mäkinen is supportedby Academy of Finland (Grant no 115340).

Corresponding author: lau@temf.tu-darmstadt.de.

SURFACE-IMPEDANCE APPROACH

The tangential electric and magnetic fields are related by a first-order SIBC of the form, $\mathbf{n}\times\mathbf{E} = Z\mathbf{n}\times(\mathbf{n}\times\mathbf{H})$, where $\mathbf{n}$ is an outward pointing normal and Z is the scalar impedance, given by $Z = \sqrt{j\omega\mu/(\sigma + j\omega\varepsilon)}$ for a lossy half plane. The impedance function is approximated in frequency domain by first-order rational functions [5],

$$Z(s) = C_0 - \sum_{p=1}^{P} C_p/(s+\alpha_p), \tag{4}$$

where P is the number of terms and α_p and C_p are the poles and coefficients of the approximation, respectively. Figure 1 shows the relative error for an approximation up to 100 THz. In time domain, recursive convolution is used for the frequency-dependent impedance [5]. In principle, any function $Z(s)$ can be considered provided the condition $\sigma >> \omega\varepsilon$ is satisfied.

The developed SIBC models are based on [5] and [6]. The loss calculation can be carried out at various stages within the nine-step procedure that constitutes a full time step of the LT scheme [3]. Due to space limitation, only the algorithms in Table 1 are discussed. Piecewise linear (denoted by A in Table 1) and piecewise constant (B) fields over the time step are considered for the recursive convolution. Algorithms 1A and 3A have separate recursion terms for longitudinal and transverse updates whereas 2B has a single recursion term updated only once per every full time step.

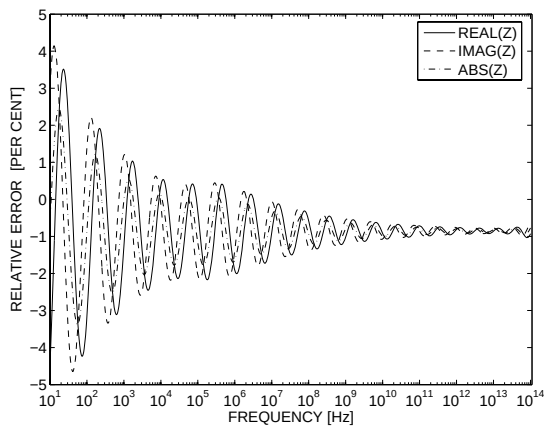

Figure 1: Relative error of a 22-term approximation of Eq. 4 at 10 Hz to 100 THz frequency band. The real part of Z primarily determines the error in the loss calculation.

Table 1: Selected SIBC Algorithms for Comparison

Description of the Algorithm	Sub steps	ID
LT-SIBC based on [6], 3 loss updates	$3 \times E\text{-}H\text{-}E$	*1A*
LT-SIBC based on [5], 1 loss update	$3 \times E\text{-}H\text{-}E$	*2B*
LT-SIBC based on [5], 3 loss updates	$3 \times H\text{-}E\text{-}H$	*3A*

The SIBC models are evaluated by calculating the quality factor Q for a 20×25×30-mm^3 rectangular cavity resonator (TM_{110} mode, wall conductivity $5.8 \cdot 10^7$ S/m). The LT scheme gives dispersion-free propagation in the longitudinal direction with the 1D magic time step which is used in all the simulations. A convergence analysis is shown in Fig. 2. Reference data calculated with CST MWS [7] eigenmode solver and the standard FIT-SIBC [5] are shown for comparison. The approximation error as shown in Fig. 1 is removed from the analysis. The accuracy of recursive convolution was found to reduce as time step was increased to 1D magic time step, however, algorithm *3A* is accurate for a wider range of grid resolutions. The error increases as approximation band width grossly exceeds simulation bandwidth due to round-off error with large values for α_p, C_p at 100 THz. Algorithm *1A* requires similar frequency range for simulation and approximation, therefore an approximation up to 20 GHz is used.

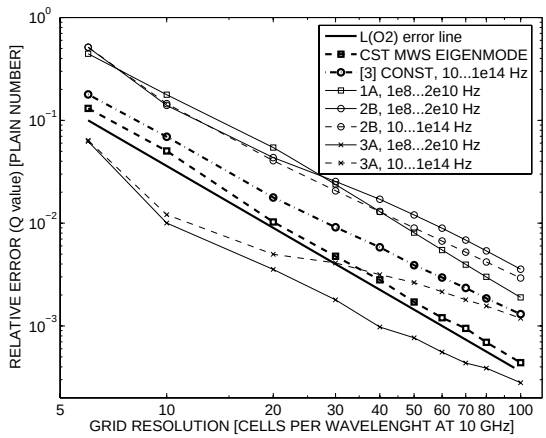

Figure 2: Relative error for Q value with respect to analytic value (Q = 11810, resonance frequency 9.598 GHz).

The situation when the grid is not aligned with geometry boundaries is investigated by considering the case of a resonator box rotated by 30° in the *xy*-plane. A convergence analysis for a rotated resonator is shown in Fig. 3. All curves show approximately first-order convergence while the relative error varies between 1-4%. The loss of 2nd convergence in this case is as expected due to the staircase approximation which is used in the present SIBC implementations.

To evaluate wide-band performance, the physical size of the resonator was varied to shift the resonance frequency between 100 Hz to 100 THz. The grid resolution remained 20 cells/λ in all simulations. The relative error is shown in Fig. 4. The error for algorithms *2B* and *3A* is similar to that in Fig. 2 (4 and 0.5%, respectively), but with the additional approximation error shown in Fig. 1.

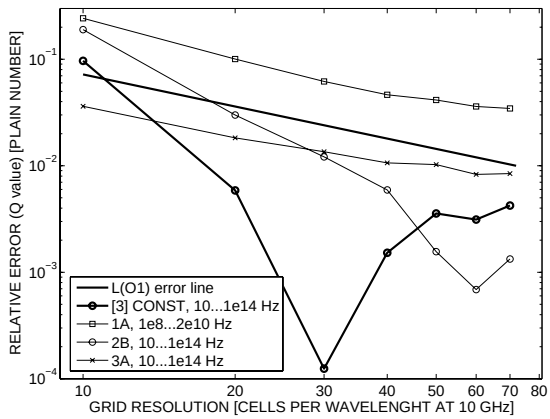

Figure 3: Same as in Fig. 2 with the resonator rotated by 30° in the *xy*-plane.

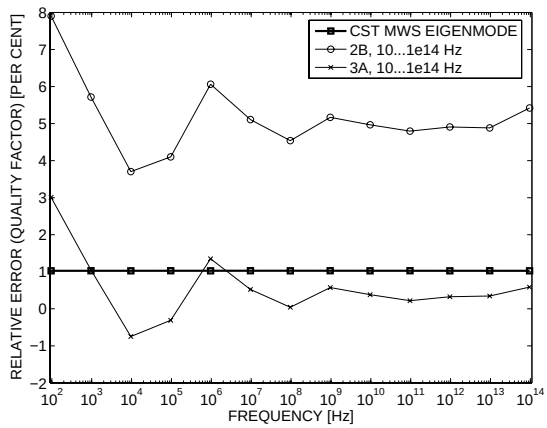

Figure 4: Relative error for Q value as a function of frequency for the wide-band approximation in Fig. 1.

WAKEFIELD SIMULATION WITH PBCI

SIBC-algorithm *2B* was implemented in the PBCI code for the purpose of wakefield computations. A first validation example consists in the calculation of resistive wakefields for a rectangular pipe containing a transition from a perfectly conducting to a finite conductivity section (see Fig. 5). A Gaussian line bunch (σ_z = 5mm, β = 1) is flying on the axis of the pipe. In order to enable a cross validation, a "full-grid" simulation taking into account the bulk conductivity of the pipe wall was performed with the CST Particle Studio® software [7]. Such a simulation, however, is only possible for unrealistically low values of conductivity, since the skin depth has to be resolved by the computational grid for all relevant frequencies. In the present case a conductivity of 3 S/m in the resistive section was assumed. Figure 6 shows the resulting longitudinal electric field in the vicinity of the bunch at a distance of 0.13m behind the transition. This electric field component represents a

purely scattered field which is only due to the resistivity of pipe walls.

The curves obtained by the two simulations agree very well. Note that the CST simulation needs a resolution of ~100 grid points per bunch length to reach the correct result. Apart from the need for resolving the skin depth this follows also from the dispersion errors which become important in the simulation of long accelerator pipes. PBCI, on the other hand converges at only 5 grid points per bunch length which is due to the application of the LT dispersion-free scheme.

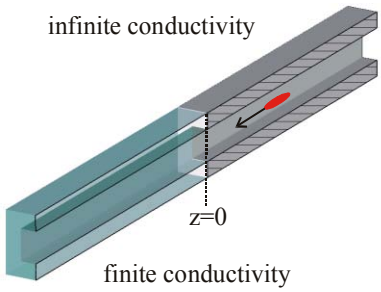

Figure 5: Bunch in a rectangular waveguide containing a transition from perfectly conducting to a resistive section at z = 0.

As a more realistic example the longitudinal wake potential for collimator #8 of the ILC-ESA test beam experiments is considered [4]. Two simulations were performed. The first one assumes perfectly conducting walls. Thus, only geometrical wakes are induced by the beam. In the second simulation, collimator walls made of titanium (with a conductivity of 6.3 106 S/m) were assumed. The longitudinal wake potentials obtained for a 1mm bunch passing through the collimator are shown in Fig. 7. Geometrical wakefields clearly dominate the solution. There is, however, an obvious resistive wake-effect. It makes up approximately 1-2% of the total wake potential in the rear of the bunch. At the present stage, this result must be still considered as preliminary. Further validation of the method is needed and will be subject of future work.

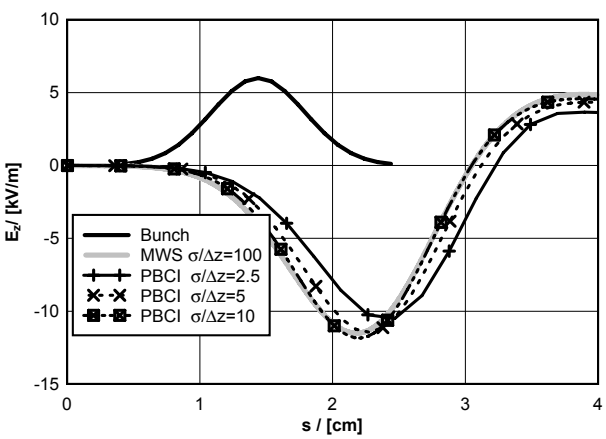

Figure 6: Longitudinal electric field on the pipe axes at 0.13m behind the transition.

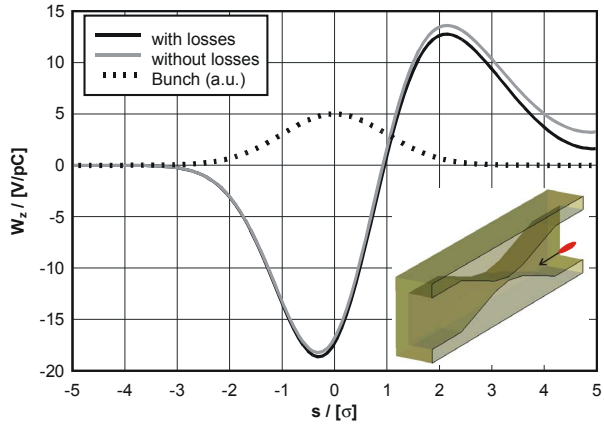

Figure 7: Longitudinal wake potential with perfectly conducting and resistive walls, respectively, for the collimator #8 of the ILC-ESA test beam experiments.

CONCLUSION

SIBC algorithms to consider frequency-dependent skin-effect loss for the dispersion-free LT scheme were introduced. One of the SIBC models was incorporated in the PBCI code and applied to wakefield simulations. Preliminary results for a simple resistive pipe example show an excellent agreement with the reference solution obtained by a commercial software. A first wakefield computation for a resistive beam collimator demonstrates the potential of the method for application in real-world simulations.

REFERENCES

[1] E. Gjonaj, X. Dong, R. Hampel, M. Kärkkäinen, T. Lau, W.F.O. Müller, and T. Weiland, "Large Scale Parallel Wake field Computations for 3D Accelerator Structures with the PBCI Code", ICAP'06, Chamonix, France, Oct. 2006, pp. 29.

[2] T. Weiland, "A Discretization Method for the Solution of Maxwell's Equations for Six-Component Fields", Int. J. Elect. Comm., Vol. 31 (1977), pp. 116.

[3] T. Lau, E. Gjonaj, T. Weiland: Time Integration Methods for Particle Beam Simulations with the Finite Integration Theory. Frequenz: Zeitschrift für Telekommunikation (FREQUENZ), Vol. 59, September 01.09.2005, pp. 210-219.

[4] N. K. Watson et al, "Direct measurements of geometric and resistive wakefields in tapered collimators for the International Linear Collider", EUROTeV-Report-2006-059 (2006).

[5] K. S. Oh and J. E. Schutt-Aine, "An Efficient Implementation of Surface Impedance Boundary Condition for the Finite-Difference Time-Domain Method", IEEE T. Antennas Propagat., (1995), pp. 660.

[6] R. M. Mäkinen, H. De Gersem, T. Weiland, and M. A. Kivikoski, "Modeling of Lossy Curved Surfaces in 3-D FIT/FDTD Techniques", IEEE T Antennas Propagat. (2006), pp. 3490.

[7] Http://www.cst.com.